ISSN: 2709-6904

JoBEF

JOURNAL OF CIVIL ENGINEERING FRONTIERS

www.jocivilef.org

New Mathematical Models for Biaxial Buckling Analysis of Thin Rectangular Plates Under Large Deflection for Various Boundary Conditions

E. I. Adah¹, H. U. Edubi² and S. U. Ubi²

¹Department of Civil and Environmental Engineering, University of Calabar, Nigeria, edwardadah@unical.edu.ng; eddytech2015@gmail.com

²Department of Civil Engineering, University of Cross River, Nigeria, (hycienthedubi@gmail.com); (emmaubi2015@yahoo.com)

Abstract

Thin rectangular plates are widely used in civil, mechanical, and aeronautical engineering, where accurate prediction of buckling behaviour is critical for structural reliability. While most classical analyses focus on small-deflection conditions, such approaches neglect the nonlinear effects induced by large out-of-plane displacements. This study aims to apply the new general mathematical model for biaxial buckling of thin isotropic plate with large deflection to formulate new specific equations for six plate boundary conditions. The nonlinear buckling behaviour is investigated for plates with boundary conditions CCCC (clamped - clamped - clamped), CSSS (clamped - simply supported - simply supported), CSCS (clamped - simply supported - clamped - simply supported), CCSS (clamped - clamped - simply supported - simply supported), CCCS (clamped - clamped - clamped - simply supported) and SSSS (simply supported all-round)) subjected to biaxial compressive loads. The new specific equations of this work allow for the evaluation of buckling load coefficients across varying aspect ratios, biaxial buckling ratios (n), and deflection-to-thickness ratios (w/t). The results obtained reveal that the biaxial buckling load coefficient (and load) decreases with increasing 'n' but increases with increase in w/t. This highlights the combined influence of loading distribution and geometric nonlinearity. Deducing from the new biaxial equations for uniaxial loading case for the purpose of comparison in square plates, the large-deflection buckling coefficients compared, showed negligible deviation (~0%) from prior works, validating the proposed equations' accuracy. Comparative analysis on values of buckling and postbuckling loads of CCCS plates against existing work under biaxial loading shows percentage differences between 0% and 5.56%, with the present results consistently upper bound but within acceptable engineering tolerances. The further comparison of biaxial buckling and posbuckling load coefficients of SSSS plate with existing works has shown also, the adequacy of this new model. The findings demonstrate that the proposed linear and nonlinear buckling equations not only aligns with established studies but also offers enhanced predictive capability for large deflection analysis of thin isotropic rectangular plates.

Keywords: Large Deflection, Buckling ratio, Biaxial in-plane Loading, Aspect Ratio, Thin isotropic plates

Received: September 05, 2025/Revised: October 16, 2025/Accepted: November 01, 2025/Online: November 08, 2025

I. INTRODUCTION

Thin plates are widely utilized across various engineering disciplines, including civil, mechanical, and aeronautical engineering, due to their structural efficiency, versatility, and ability to carry significant loads relative to their weight [1]. In many applications, these plates are subjected to in-plane compressive forces arising from structural loads, thermal stresses, or aerodynamic pressures [2]. Such compressive forces induce deflections in the plate, which, under small load magnitudes, may remain within the elastic range and cause only minor displacements [3], [4]. However, with the continuous or progressive application of compressive loads, these deflections can increase substantially, leading to large displacement behaviour [5]. At this stage, nonlinear geometric effects become

significant, and the plate's stiffness, stability, and load-carrying capacity may be considerably affected, necessitating advanced analytical or numerical methods for accurate modelling and safe design [6]. When the deflection of a thin plate becomes comparable to its thickness, the structural response transit from a linear to a nonlinear regime [7]. In this state, the assumptions underlying the classical Kirchhoff plate theory, particularly the neglect of in-plane stretching of the plate's middle surface, are no longer valid [8].

The deformation induces significant membrane stresses in the middle surface, which interact with bending effects, thereby altering the overall stiffness and load distribution of the plate [9]. To accurately capture this nonlinear behaviour, the analysis must account for both bending and stretching actions, leading to the development of more complex governing equations [10],



[11], [12]. A foundational contribution in this regard was made by Von Kármán in 1910, who formulated a set of nonlinear plate equations based on Airy's stress functions [13], [14]. While these equations provide a rigorous theoretical framework for modelling large deflections, their coupled and highly nonlinear nature makes manual computation extremely tedious, often necessitating numerical methods or computational techniques for practical applications. Over the years, numerous scholars [15], [16], [17] have investigated the buckling behaviour of rectangular thin plates under small deflections for both uniaxial and biaxial loading conditions, employing a variety of analytical and approximate techniques. Among these, the Galerkin method and the Ritz method, both rooted in the principles of energy methods, have been widely recognized for their effectiveness in predicting buckling loads and modes for such structural elements [18], [19], [20]. These approaches leverage variational formulations to provide accurate and computationally efficient solutions for plates subjected to different loading scenarios and boundary configurations. On large deflection analysis, Levy [21] made a great classical attempt in solving the von Karman large deflection equations using assumed trigonometric shape function for a plate simply supported all-round (SSSS) only subjected to uniaxial in-plane loads. His work provided the first basic solution approach and numerical values for further research validation.

Recent works on large deflection of thin plates had been carried out by some scholars among them is [22] who carried out a direct integration of the two von Karman large deflection equations for a uniaxially loaded thin plates. He employed the polynomial displacement shape function to obtain the solution to the buckling and post buckling problem of thin plates. However, this great attempt was still based directly on the von Karman 4th order partial differential equations with the involvement of Airy's stress functions and with serious computational complexities especially for manual computation. To avert the continuous dependence on the von Karman 1910 equation of large deflection with it accompanied difficulties, [16], [23] formulated an improved alternative mathematical model for large deflection analysis of thin isotropic plates subjected to uniaxial buckling completely devoid of the Airy's stress function in particular and von Karman equations in general. This equation has been applied to a wide range of boundary conditions using both the trigonometric and polynomial displacement shape functions with very high degree of accuracy. It is clear that there is no simple equation for biaxial buckling analysis of thin plates with large deflection for these boundary conditions. Hence, building upon this body of knowledge and effort, [24] in his master's thesis submitted to the department of civil engineering, university of Cross River, extended the works of [23] to biaxial buckling by formulating a general equation (Equation 2.5) for analysis of thin isotropic plates with large deflection.

The present study aimed to apply this general equation to formulate new specific equations for six boundary conditions of thin plates, and evaluating the buckling characteristics of thin rectangular plates subjected to biaxial compressive forces under large deflection. This would be done by choosing suitable polynomial shape functions and evaluating the bending, membrane and geometric stiffness of the six plates considered.

And using the general equation to obtain the new specific equation for each plate under consideration. Remember, unlike small-deflection analyses where material and geometric nonlinearities are negligible, this work incorporates the influence of membrane forces that develop in the plate's middle surface as a direct consequence of significant out-of-plane displacements.

The investigation considers a range of boundary conditions, including CCCC (clamped - clamped - clamped). CSSS (clamped - simply supported - simply supported - simply supported), CSCS (clamped - simply supported - clamped simply supported), CCSS (clamped - clamped - simply supported - simply supported), CCCS (clamped - clamped clamped - simply supported), and SSSS (Simply supported at four edges), to comprehensively assess how this general equation is suitable for plate stability analysis and assess how edge restraints influence the plate's buckling and postbuckling response. This analysis provides deeper insight into the interplay between boundary conditions, large deflection effects, and biaxial loading, thereby extending the applicability of existing buckling theories to more realistic engineering scenarios. The outcome of this work will provide relevant information on the suitability of the new model, present new simple specific mathematical models, provide relevant numerical data for research and design, and deepen understanding of thin rectangular isotropic plates subjected to biaxial in-plane loading. These contributions will improve design safety and avert economic waste.

II. THE TOTAL POTENTIAL ENERGY FUNCTIONAL FOR A RECTANGULAR PLATE UNDER BIAXIAL IN-PLANE LOADING

The Ritz total potential energy functional, Π of thin rectangular plates under large displacement subjected to uniaxial in-plane loading as given by [23] is

$$\begin{split} \Pi &= \frac{D}{2} \int_{0}^{a} \int_{0}^{b} \left[\left(\frac{\partial^{2} w}{\partial x^{2}} \right)^{2} + 2 \left(\frac{\partial^{2} w}{\partial x \partial y} \right)^{2} + \left(\frac{\partial^{2} w}{\partial y^{2}} \right)^{2} \right] dx dy \\ &\quad + \frac{gD}{2*16} \int_{0}^{a} \int_{0}^{b} \left[\left(\frac{\partial w}{\partial x} \right)^{4} + 2 \left(\frac{\partial w}{\partial x} \right)^{2} \left(\frac{\partial w}{\partial y} \right)^{2} \\ &\quad + \left(\frac{\partial w}{\partial y} \right)^{4} \right] dx dy \\ &\quad - \frac{1}{2} \int_{0}^{a} \int_{0}^{b} N_{x} \left(\frac{\partial w}{\partial x} \right)^{2} dx dy \end{split} \tag{1}$$

For plate with biaxial in-plane loading, [24] modified (1) to (2)

$$\begin{split} \Pi &= \frac{D}{2} \int_{0}^{a} \int_{0}^{b} \left[\left(\frac{\partial^{2} w}{\partial x^{2}} \right)^{2} + 2 \left(\frac{\partial^{2} w}{\partial x \, \partial y} \right)^{2} + \left(\frac{\partial^{2} w}{\partial y^{2}} \right)^{2} \right] dx dy \\ &+ \frac{gD}{32} \int_{0}^{a} \int_{0}^{b} \left[\left(\frac{\partial w}{\partial x} \right)^{4} + 2 \left(\frac{\partial w}{\partial x} \right)^{2} \left(\frac{\partial w}{\partial y} \right)^{2} \right. \\ &+ \left(\frac{\partial w}{\partial y} \right)^{4} \right] dx dy \\ &- \frac{1}{2} \int_{0}^{a} \int_{0}^{b} \left[N_{x} \left(\frac{\partial w}{\partial x} \right)^{2} \right. \\ &+ 2 N_{xy} \left(\frac{\partial w}{\partial y} \right) \left(\frac{\partial w}{\partial y} \right) \\ &+ N_{y} \left(\frac{\partial w}{\partial y} \right)^{2} \right] dx dy \end{split} \tag{2}$$

Where:

w = Out of Plane Displacement; D = Flexural rigidity of theplate; N_x = In-plane force along the x – axis, N_v = Inplane force along the y – axis.

$$D = \frac{Et^3}{12(1-v^2)}; g = \frac{12}{t^2}; \frac{Et}{1-v^2}$$

= gD; (3a, b, c)

Using the non-dimensional parameter,

$$x = aR$$
; $y = bQ$; for $0 \le R \le 1$ and $0 \le Q \le 1$

This equation incorporates both geometric and material nonlinearities.

From (2), Edubi [24] formulated a new general biaxial buckling equation for thin rectangular plate with large displacement as given in (5)

$$N_{x} = \frac{\left[K_{bT} + \frac{3}{2} \frac{1}{(h_{max})^{2}} \left(\frac{w}{t}\right)^{2} K_{mT}\right]}{\left[K_{Nx} + \frac{nK_{Ny}}{2^{2}}\right]} \frac{D}{a^{2}}$$
(5)

Where h_{max} is the value of the shape profile at point of maximum deflection.

n is the load factor given as

$$n = \frac{Ny}{Ny} \tag{6}$$

$$k_{bT} = K_{bx} + \frac{2}{2^2} K_{bxy} + \frac{1}{2^4} K_{by}$$
 (7)

$$k_{mT} = K_{mx} + \frac{2}{2^2} K_{mxy} + \frac{k_{my}}{2^4}$$
 (8)

 k_{bT} = Total bending stiffness

 k_{mT} = Total membrane stiffness

 k_{bx} = Bending stiffness along x – axis given as

$$k_{bx} = \int_0^1 \int_0^1 \left(\frac{\partial^2 h}{\partial R^2}\right)^2 dRdQ \tag{9}$$

$$k_{bxy} = \int_0^1 \int_0^1 \left(\frac{\partial^2 h}{\partial R \partial Q} \right)^2 dR dQ \qquad (10)$$

$$k_{by} = \text{Bending stiffness along } y - \text{axis given as}$$

$$k_{by} = \int_0^1 \int_0^1 \left(\frac{\partial^2 h}{\partial Q^2}\right)^2 dRdQ \tag{11}$$

$$k_{mx} = \int_0^1 \int_0^1 \left(\frac{\partial h}{\partial R}\right)^4 dR dQ$$
 (12)

$$k_{\text{mxy}} = \int_0^1 \int_0^1 \left(\frac{\partial h}{\partial R}\right)^2 \left(\frac{\partial h}{\partial Q}\right)^2 dRdQ \qquad (13)$$

$$k_{my} = \int_0^1 \int_0^1 \left(\frac{\partial h}{\partial Q}\right)^4 dRdQ$$
 (14)

$$k_{Nx} = \text{Geometric stiffness along } x - \text{axis given as}$$

$$k_{Nx} = \int_0^1 \int_0^1 \left(\frac{\partial h}{\partial R}\right)^2 dRdQ \qquad (15)$$

 k_{Nxy} = Geometric stiffness along xy – axis given as

$$k_{\text{Nxy}} = \int_0^1 \int_0^1 \left(\frac{\partial h}{\partial R}\right) \left(\frac{\partial h}{\partial Q}\right) dRdQ$$
 (16)

$$k_{Ny} = \int_0^1 \int_0^1 \left(\frac{\partial h}{\partial Q}\right)^2 dRdQ \tag{17}$$

R = Non dimensional parameter along x - directionQ = Non dimensional parameter along x - directionh =the shape profile of the plate

$$2 = \frac{b}{a}$$
 is the aspect ratio (18)
From (5),

$$\eta_{Lx} = \frac{\left[K_{bT} + \frac{3}{2} \frac{1}{(h_{max})^2} \left(\frac{w}{t}\right)^2 K_{mT}\right]}{\left[K_{Nx} + \frac{nK_{Ny}}{2^2}\right]} \frac{D}{a^2}$$
(19)

This is the coefficient of biaxial buckling load for thin rectangular plates under large displacement.

Hence, (5) becomes
$$N_x = \eta_{Lx} \frac{D}{r^2}$$
(20)

Determining the Stiffnesses for the Rectangular Plate in this study

The governing differential equation of a plate is given by [13] as

$$\left[\left(\frac{\partial^2 \mathbf{w}}{\partial \mathbf{x}^2} \right)^2 + 2 \left(\frac{\partial^2 \mathbf{w}}{\partial \mathbf{x} \, \partial \mathbf{y}} \right)^2 + \left(\frac{\partial^2 \mathbf{w}}{\partial \mathbf{y}^2} \right)^2 \right] - \frac{q}{D} \quad (21)$$

In an attempt for find solution to (21), [25], [26] carried out a direct integration of the governing partial differential equation of a plate in Equation (21) to obtain the general deflected shape function, w, of a rectangular plate in a compacted series form as

$$w = \sum_{m=0}^{m} \sum_{n=0}^{n} \alpha_m R^m \beta_n Q^n$$
 (22)

Equation (22) is a power series equation where α_m and β_n are constants of the series; R and Q are nondimensional parameters along x- and y- axes respectively; and m and n are the powers of the series along x- and y-axes respectively. They expressed the series equation in (22) in an expanded form as a truncated power series equation given in (23) as

$$w = (\alpha_0 + \alpha_1 R + \alpha_2 R^2 + \alpha_3 R^3 + \alpha_4 R^4)(\beta_0 + \beta_1 Q + \beta_2 Q^2 + \beta_3 Q^3 + \beta_4 Q^4)$$
 (23)

To determine the constants α and β , [26] applied the boundary conditions to a rectangular plate using (2.23) to obtain the polynomial deflected shape function for the plate types considered in this work as given in Table 1. These polynomial shape functions satisfy the geometric condition along the edge by having zero deflection at all the edges. Also, these deflected shape functions are very simple and easy to differentiate and integrate compared to the assumed trigonometric shape functions or Fourier series functions used by previous authors. Moreso, the results obtained with these polynomial shape functions for previous works on bending, buckling and vibration analyses of rectangular plates with small and large deflections [27], [28], [29], [30], [31], [16] were very adequate.

TABLE 1: THE POLYNOMIAL DISPLACEMENT SHAPE PROFILE, H. SOURCE: [26]

DI 4 T	Deflected Shape Function, w =Ah
Plate Type	h
CCCC	$(R^2 - 2R^3 + R^4)(Q^2 - 2Q^3 + Q^4)$
CSSS	$(R - 2R^3 + R^4)(1.5Q^2 - 2.5Q^3 + Q^4)$
CSCS	$(R - 2R^3 + R^4)(Q^2 - 2Q^3 + Q^4)$
CCSS	$(1.5R^2 - 2.5R^3 + R^4)(1.5Q^2 - 2.5Q^3 + Q^4)$
CCCS	$(1.5R^2 - 2.5R^3 + R^4)(Q^2 - 2Q^3 + Q^4)$
SSSS	$(R - 2R^3 + R^4)(Q - 2Q^3 + Q^4)$

To determine the stiffness of each of these plate types considered here, these polynomial deflected shape function given in Table 1 for the CCCC, CSSS, CSCS, CCSS, CCCS and SSSS plates types were used. The stiffnesses for CCCC, CSSS, CSCS, CCSS, CCCS and SSSS were calculated using (9) to (17) by substituting their specific shape profile as given in Table 1, and the results obtained are presented in Tables 2-4.

Substituting the stiffness values in Tables 2 into (7) and (8) yields the total bending stiffness and membrane stiffness expression for the various boundary conditions under consideration.

Evaluating the maximum value of h for all the boundary conditions

The point of maximum deflection of these plates is at the middle of the plate for all boundary conditions considered, and this corresponds to R = Q = 0.5. Hence, substituting this value of R and Q into each profile in Table 1 and evaluating yields the results presented in Table 5.

The New Specific Equations

In order to obtain the specific equation for each plate type considered, the stiffness values in Tables 2-4 and the h_{max} values in Table 5 for each plate boundary condition were substituted into (5) to get the new specific biaxial buckling equation of the respective rectangular plates under large deflection as shown in Table 6.

III. RESULTS

The results obtained from section 2 are presented in Tables 2 - 6.

TABLE 2: SUMMARY OF BENDING STIFFNESS VALUES

PLATE TYPE	K _{bx}	K _{bxy}	K_{by}
CCCC	0.0012698413	0.0003628118	0.0012698413
CSSS	0.0361904762	0.0416326531	0.0885714286
CSCS	0.0076190476	0.0092517007	0.0393650794
CCSS	0.0135714286	0.0073469388	0.0135714286
CCCS	0.0028571429	0.0016326531	0.0060317460
SSSS	0.2361904762	0.2359183673	0.2361904762

TABLE 3: SUMMARY OF MEMBRANE STIFFNESS VALUES

PLATE TYPE	K _{mx}	K _{mx} K _{mxy}			
CCCC	0.0000000024	0.0000000005	0.0000000024		
CSSS	0.0000340978	0.0000045749	0.0000449254		
CSCS	0.0000016447	0.0000002610	0.0000019245		
CCSS	0.0000011786	0.0000001515	0.0000011786		
CCCS	0.0000000568	0.0000000086	0.0000000505		
SSSS	0.0012997694	0.0001381780	0.0012997694		

TABLE 4: SUMMARY OF GEOMETRIC LOAD STIFFNESS VALUES

S/N	PLATE TYPE	K _{Nx}	K_{Ny}
1	CCCC	0.0000302343	0.0000302343
2	CSSS	0.0036621315	0.0042176871
3	CSCS	0.0007709751	0.0009372638
4	CCSS	0.0006462585	0.0006462585
5	CCCS	0.0001360544	0.0001436130
6	SSSS	0.0239002268	0.0239002268

TABLE 5: Values of the Maximum Shape Profile, HMAX at (R = Q = 0.5)

BCs	CCCC	CSSS	CSCS	CCSS	CCCS
h _{max}	0.00390625	0.0390625	0.01953125	0.015625	0.0078125

TABLE 6: New Biaxial Buckling Load Equation Under Large Deflection for Rectangular Plates in this study (ie Buckling and Postbuckling Equations)

PLATE TYPE	$ \begin{aligned} \textbf{Biaxial Buckling Load Equation, N}_{x} &= \eta_{Lx} \frac{D}{a^{2}} = \frac{\left[K_{bT} + \frac{3}{2} \frac{1}{(h_{max})^{2}} \left(\frac{w}{t}\right)^{2} K_{mT}\right]}{\left[K_{NX} + \frac{nK_{Ny}}{2^{2}}\right]} \frac{D}{a^{2}} \end{aligned} $
CCCC	$\frac{\left[\left(0.0012698413 + \frac{0.0007256236}{2^2} + \frac{0.0012698413}{2^4}\right) + \left(\frac{w}{t}\right)^2 \left(0.0002393913 + \frac{0.0000968965}{2^2} + \frac{0.0002393913}{2^4}\right)\right]}{\left[0.0000302343 + \frac{0.0000302343n}{2^2}\right]} \cdot \frac{D}{a^2}$
CSSS	$\frac{\left[\left(0.0361904762+\frac{0.0832653062}{2^2}+\frac{0.0885714286}{2^4}\right)+\left(\frac{w}{t}\right)^2\left(0.0335195010+\frac{0.0089947035}{2^2}+\frac{0.0441634636}{2^4}\right)\right]}{\left[0.0036621315+\frac{0.0042176871n}{2^2}\right]}\cdot\frac{D}{a^2}$
CSCS	$\frac{\left[\left(0.0076190476 + \frac{0.0185034014}{2^2} + \frac{0.0393650794}{2^4}\right) + \left(\frac{w}{t}\right)^2 \left(0.0064671561 + \frac{0.0020522675}{2^2} + \frac{0.0075675011}{2^4}\right)\right]}{\left[0.0007709751 + \frac{0.0009372638n}{2^2}\right]} \cdot \frac{D}{a^2}$
CCSS	$\frac{\left[0.0007/09751 + \frac{2^{2}}{2^{2}}\right]}{\left[\left(0.0135714286 + \frac{0.0146938776}{2^{2}} + \frac{0.0135714286}{2^{4}}\right) + \left(\frac{w}{t}\right)^{2}\left(0.0072410777 + \frac{0.0018612889}{2^{2}} + \frac{0.0072410777}{2^{4}}\right)\right]}{\left[0.0006462585 + \frac{0.0006462585n}{2^{2}}\right]}.\frac{D}{a^{2}}$
CCCS	$\frac{\left[0.0006462585 + \frac{1}{2^2}\right]}{\left[\left(0.0028571429 + \frac{0.0032653062}{2^2} + \frac{0.0060317460}{2^4}\right) + \left(\frac{w}{t}\right)^2 \left(0.0013970727 + \frac{0.0004246791}{2^2} + \frac{0.0012407737}{2^4}\right)\right]}{\left[0.0001360544 + \frac{0.0001436130n}{2^2}\right]} \cdot \frac{D}{a^2}$
SSSS	$\frac{\left[0.0001360544 + \frac{0.0001360544}{2^2}\right]}{\left[\left(0.2361904762 + \frac{0.4718367346}{2^2} + \frac{0.2361904762}{2^4}\right) + \left(\frac{w}{t}\right)^2 \left(0.2044360431 + \frac{0.0434670247}{2^2} + \frac{0.2044360431}{2^4}\right)\right]}{\left[0.0239002268 + \frac{0.0239002268n}{2^2}\right]} \cdot \frac{D}{a^2}$

Using the derived equations or mathematical models in Table 6, the biaxial buckling load coefficients for rectangular plates under large deflection for various boundary conditions can be evaluated for various aspect ratios and biaxial buckling ratios.

For instance, considering a square plate for each of these boundary conditions with a biaxial buckling load ratio, n, ranging from 0 to 1.0 at intervals of 0.1, and a deflection-to-thickness ratio, w/t, ranging from 0 to 1.0 at intervals of 0.1, we have the numerical values of the coefficient of biaxial buckling load under large displacement as presented in Tables 7 to 12.

TABLE 7: BIAXIAL BUCKLING LOAD COEFFICIENT FOR CCCC PLATE WITH ASPECT RATIO OF $1.0\,$

		η_{Lx}												
n w/t	0	0.1	0.2	0.3	0.4	0.5	0.6	0.7	0.8	0.9	1			
0	108.000	98.182	90.000	83.077	77.143	72.000	67.500	63.529	60.000	56.842	54.000			
0.1	108.190	98.355	90.159	83.223	77.279	72.127	67.619	63.641	60.106	56.942	54.095			
0.2	108.762	98.874	90.635	83.663	77.687	72.508	67.976	63.977	60.423	57.243	54.381			
0.3	109.714	99.740	91.428	84.395	78.367	73.142	68.571	64.537	60.952	57.744	54.857			

Adah et al. / Journal of Civil Engineering Frontiers Vol. 06, No. 02, pp. 103 –115, (2025)

0.4	111.047	100.951	92.539	85.420	79.319	74.031	69.404	65.322	61.693	58.446	55.523
0.5	112.760	102.509	93.967	86.739	80.543	75.173	70.475	66.330	62.645	59.347	56.380
0.6	114.855	104.413	95.712	88.350	82.039	76.570	71.784	67.562	63.808	60.450	57.427
0.7	117.330	106.664	97.775	90.254	83.807	78.220	73.331	69.018	65.183	61.753	58.665
0.8	120.186	109.260	100.155	92.451	85.847	80.124	75.116	70.698	66.770	63.256	60.093
0.9	123.423	112.203	102.852	94.941	88.159	82.282	77.139	72.602	68.568	64.959	61.711
1	127.041	115.492	105.867	97.724	90.743	84.694	79.400	74.730	70.578	66.864	63.520

TABLE 8: BIAXIAL BUCKLING LOAD COEFFICIENT FOR CSSS PLATE WITH ASPECT RATIO OF 1.0

						η_{Lx}					
n w/t	0	0.1	0.2	0.3	0.4	0.5	0.6	0.7	0.8	0.9	1
0	56.805	50.938	46.170	42.218	38.889	36.047	33.592	31.450	29.565	27.893	26.400
0.1	57.042	51.151	46.362	42.394	39.051	36.197	33.732	31.581	29.688	28.009	26.510
0.2	57.752	51.787	46.940	42.922	39.538	36.648	34.152	31.974	30.058	28.358	26.840
0.3	58.935	52.849	47.901	43.801	40.348	37.399	34.852	32.629	30.674	28.939	27.390
0.4	60.592	54.334	49.248	45.033	41.482	38.450	35.832	33.547	31.536	29.753	28.160
0.5	62.722	56.244	50.979	46.616	42.940	39.802	37.091	34.726	32.645	30.798	29.150
0.6	65.326	58.579	53.096	48.551	44.723	41.454	38.631	36.168	34.000	32.077	30.360
0.7	68.403	61.338	55.596	50.838	46.829	43.407	40.450	37.871	35.601	33.588	31.790
0.8	71.953	64.522	58.482	53.476	49.260	45.660	42.550	39.837	37.449	35.331	33.440
0.9	75.977	68.130	61.752	56.467	52.014	48.213	44.929	42.064	39.543	37.307	35.310
1	80.474	72.163	65.408	59.809	55.093	51.067	47.589	44.554	41.884	39.515	37.400

TABLE 9: BIAXIAL BUCKLING LOAD COEFFICIENT FOR CSCS PLATE WITH ASPECT RATIO OF $1.0\,$

		-				η_{Lx}					
n w/t	0	0.1	0.2	0.3	0.4	0.5	0.6	0.7	0.8	0.9	1
0	84.941	75.734	68.328	62.241	57.150	52.829	49.116	45.890	43.062	40.562	38.336
0.1	85.150	75.920	68.496	62.394	57.291	52.959	49.236	46.003	43.167	40.661	38.430
0.2	85.776	76.478	68.999	62.853	57.712	53.348	49.598	46.341	43.485	40.960	38.713
0.3	86.819	77.409	69.839	63.617	58.414	53.997	50.202	46.904	44.014	41.459	39.184
0.4	88.280	78.711	71.014	64.688	59.397	54.906	51.046	47.693	44.754	42.156	39.843
0.5	90.158	80.385	72.524	66.064	60.660	56.074	52.132	48.708	45.706	43.053	40.691
0.6	92.453	82.432	74.371	67.746	62.204	57.501	53.459	49.948	46.870	44.149	41.726
0.7	95.165	84.850	76.553	69.733	64.029	59.188	55.028	51.413	48.245	45.444	42.951
0.8	98.295	87.641	79.070	72.027	66.135	61.135	56.837	53.104	49.832	46.939	44.363
0.9	101.842	90.804	81.924	74.626	68.522	63.341	58.888	55.021	51.630	48.633	45.964
1	105.807	94.338	85.113	77.531	71.189	65.807	61.181	57.163	53.640	50.526	47.754

TABLE 10: BIAXIAL BUCKLING LOAD COEFFICIENT FOR CCSS PLATE WITH ASPECT RATIO OF $1.0\,$

_						η_{Lx}					
n w/t	0	0.1	0.2	0.3	0.4	0.5	0.6	0.7	0.8	0.9	1
0	64.737	58.852	53.947	49.798	46.241	43.158	40.461	38.080	35.965	34.072	32.368
0.1	64.990	59.082	54.158	49.992	46.421	43.326	40.619	38.229	36.105	34.205	32.495
0.2	65.748	59.771	54.790	50.576	46.963	43.832	41.093	38.676	36.527	34.604	32.874
0.3	67.013	60.921	55.844	51.548	47.866	44.675	41.883	39.419	37.229	35.270	33.506
0.4	68.783	62.530	57.319	52.910	49.131	45.855	42.989	40.461	38.213	36.202	34.392
0.5	71.059	64.599	59.216	54.661	50.757	47.373	44.412	41.800	39.477	37.400	35.530
0.6	73.841	67.128	61.534	56.801	52.744	49.227	46.151	43.436	41.023	38.864	36.921
0.7	77.129	70.117	64.274	59.330	55.092	51.419	48.205	45.370	42.849	40.594	38.564
0.8	80.922	73.565	67.435	62.248	57.801	53.948	50.576	47.601	44.957	42.591	40.461
0.9	85.221	77.474	71.018	65.555	60.872	56.814	53.263	50.130	47.345	44.853	42.611
1	90.026	81.842	75.022	69.251	64.304	60.017	56.266	52.957	50.015	47.382	45.013

TABLE 11: BIAXIAL BUCKLING LOAD COEFFICIENT FOR CCCS PLATE WITH ASPECT RATIO OF 1.0

						η_{Lx}					
n w/t	0	0.1	0.2	0.3	0.4	0.5	0.6	0.7	0.8	0.9	1
0	89.333	80.804	73.761	67.848	62.813	58.473	54.694	51.374	48.434	45.812	43.459
0.1	89.558	81.008	73.947	68.019	62.971	58.620	54.832	51.503	48.556	45.927	43.569
0.2	90.234	81.618	74.505	68.532	63.446	59.062	55.245	51.892	48.922	46.274	43.897
0.3	91.359	82.636	75.434	69.387	64.237	59.799	55.934	52.539	49.532	46.851	44.445
0.4	92.935	84.062	76.735	70.583	65.345	60.830	56.899	53.445	50.386	47.659	45.212
0.5	94.961	85.894	78.408	72.122	66.769	62.156	58.139	54.610	51.485	48.698	46.197
0.6	97.437	88.134	80.452	74.003	68.510	63.777	59.655	56.034	52.827	49.968	47.402
0.7	100.363	90.781	82.869	76.225	70.568	65.692	61.447	57.717	54.414	51.468	48.825
0.8	103.739	93.835	85.656	78.789	72.942	67.902	63.514	59.658	56.244	53.200	50.468
0.9	107.566	97.296	88.816	81.696	75.632	70.407	65.857	61.859	58.319	55.162	52.329
1	111.843	101.164	92.347	84.944	78.640	73.206	68.475	64.319	60.638	57.355	54.410

TABLE 12: BIAXIAL BUCKLING LOAD COEFFICIENT FOR SSSS PLATE WITH ASPECT RATIO OF $1.0\,$

						η_{Lx}					
n w/t	0	0.1	0.2	0.3	0.4	0.5	0.6	0.7	0.8	0.9	1
0	39.507	35.915	32.922	30.390	28.219	26.338	24.692	23.239	21.948	20.793	19.753
0.1	39.696	36.087	33.080	30.535	28.354	26.464	24.810	23.351	22.053	20.893	19.848
0.2	40.264	36.603	33.553	30.972	28.760	26.842	25.165	23.685	22.369	21.191	20.132
0.3	41.210	37.464	34.342	31.700	29.436	27.473	25.756	24.241	22.894	21.689	20.605
0.4	42.535	38.668	35.446	32.719	30.382	28.357	26.584	25.020	23.630	22.387	21.267

0.5	44.238	40.217	36.865	34.029	31.599	29.492	27.649	26.022	24.577	23.283	22.119
0.6	46.320	42.109	38.600	35.631	33.086	30.880	28.950	27.247	25.733	24.379	23.160
0.7	48.780	44.346	40.650	37.523	34.843	32.520	30.488	28.694	27.100	25.674	24.390
0.8	51.619	46.927	43.016	39.707	36.871	34.413	32.262	30.364	28.677	27.168	25.810
0.9	54.837	49.852	45.697	42.182	39.169	36.558	34.273	32.257	30.465	28.861	27.418
1	58.433	53.121	48.694	44.948	41.738	38.955	36.520	34.372	32.463	30.754	29.216

w/t = deflection to thickness ratio; n = biaxial loading ratio.

DISCUSSIONS OF RESULTS

The specific mathematical models from this work presented in Table 6 indicates that the biaxial buckling of a plate comprises of the bending and membrane stiffness terms. Also, it shows that the membrane term is dependent on the deflection of the plate as a result of the in-plane load. Moreso, in terms of design, the biaxial buckling load is a function of three parameters only, namely the aspect ratio of the plate, the flexural rigidity and the length of the plate along the x-axis. This makes the models very simple and easy to apply in plate stability analysis and design, as these parameters can easily be determined from the practical or design requirements by the designer. The aspect ratio can be determined from the selected plate dimensions; the flexural rigidity is easily obtained from the type of material used (which has its Poisson ratio and Young's modulus). Therefore, the biaxial buckling load of these plates can be predicted without difficulties. Also, the specific models can be used to predict the critical load of a plate (small deflection) when w/t equals zero; at this point the plate has no deflection. The models can also be used to predict the uniaxial buckling load of plates under large displacement when the buckling factor, n, is set to zero. Hence, these new models are all-encompassing, which is an added advantage and merit of the models.

To understand the behaviour of the plates, numerical results presented in Tables 5 to 10 were generated. From the results, the biaxial buckling load coefficient for the various rectangular plate

configurations exhibited a decreasing trend with increasing biaxial buckling ratio, n. This means that as the loadings in both directions approach each other in magnitude, the strength of the plate reduces, and the plate is more prone to failure. In contrast, the results demonstrate an increasing strength of the plates as the deflection-to-thickness ratio, w/t, rises. This is due to stiffening or hardening of the plates beyond initial yield point. This implies that rectangular plates do not fail at the initial yield point as columns do. Plates possess extra strength beyond the initial yield point. This point gives rise to enhanced economic approach to design. Hence, one can saves material wastage and reduces the cost of the project. In addition, the implication of these results to design is that, when a plate is subjected to biaxial in-plane loading, it reaches its ultimate yield point faster or easily than when it is uniaxially loaded. As a result of this, plates subjected to biaxial loading fail easily than those subjected to uniaxial loading. Hence, designers of plate must understand the loading condition of a plate in order to avert structural failure and economic waste. The new equations are unique and only applicable to the respective boundary conditions or plate types.

To validate the models, a comparison was made with the values in literature. The uniaxial buckling coefficient results for large deflection/displacement in CCCC, CSSS, CSCS, CCSS, CCCS and SSSS plates are compared with those reported by [23], as presented in Table 13.

TABLE 13: COMPARISON OF UNIAXIAL BUCKLING LOAD COEFFICIENT RESULTS FOR LARGE DEFLECTION/DISPLACEMENT

		η_{Lx}											
PLATE TYPE	w/t	0	0.25	0.5	0.75	1	1.25	1.5	1.75	2			
	Present Study	108.000	109.190	112.760	118.710	127.041	137.751	150.841	166.312	184.162			
CCCC	Adah et al. (2023)	108	109.19	112.76	118.71	127.041	137.751	150.841	166.312	184.162			
	Percentage Difference	0.00006	0.00009	0.000185	0.00033	-0.0003	-0.000006	0.00027	-0.00007	0.00024			
	Present Study	56.805	58.284	62.722	70.119	80.474	93.787	110.059	129.290	151.480			
CSSS	Adah et al. (2023)	56.805	58.285	62.726	70.128	80.491	93.814	110.098	129.343	151.549			
	Percentage Difference	-0.00008	-0.0013	-0.006196	-0.0135	-0.0216	-0.0286	-0.0351	-0.0409	-0.0459			
	Present Study	84.941	86.245	90.158	96.678	105.807	117.544	131.889	148.842	168.404			
CSCS	Adah et al. (2023)	84.941	86.245	90.158	96.678	105.807	117.544	131.889	148.843	168.404			
	Percentage Difference	0.0002	0.000321	-0.000452	0.00012	-0.0001	-0.0002	-0.00003	-0.0004	-0.00005			
CCCC	Present Study	64.737	66.317	71.059	78.962	90.026	104.251	121.638	142.185	165.894			
CCSS	Adah et al. (2023)	64.737	66.317	71.059	78.962	90.026	104.251	121.638	142.185	165.894			

	Percentage Difference	-0.0002	0.000642	0.0002463	0.00011	0.00019	0.0004	-0.0001	0.00029	0.0001
cccs	Present Study	89.333	90.740	94.961	101.995	111.843	124.505	139.980	158.269	179.372
	Adah et al. (2023)	89.333	90.74	94.961	101.995	111.843	124.505	139.98	158.269	179.372
	Percentage Difference	0.00039	0.000215	-0.000276	-0.00002	-0.00008	-0.0004	-0.00009	-0.00007	-0.0002

The uniaxial buckling analysis under large deflection for square plates (aspect ratio of 1.0) with deflection-to-thickness ratios (w/t) ranging from 0 to 2.0 in increments of 0.25 exhibits negligible variation, practically 0%, when compared with the results of [23] for the boundary conditions CCCC, CSSS, CSCS, CCSS, and CCCS. The minor variation is due to approximation numerical values especially number of decimal places from the stiffness value used. This high degree of correlation not only validates the accuracy of the proposed buckling load equation but also confirms its robustness and wide applicability of the (5) across a range of plate types.

In addition, Figure 1 presents a comparative analysis of the biaxial buckling load coefficient for a CCCS square plate, with the results of [17], who carried out small deflection analysis on biaxial buckling of plates using the Galerkin method for biaxial buckling ratio (n) values ranging from 0 to 1 in increments of 0.1

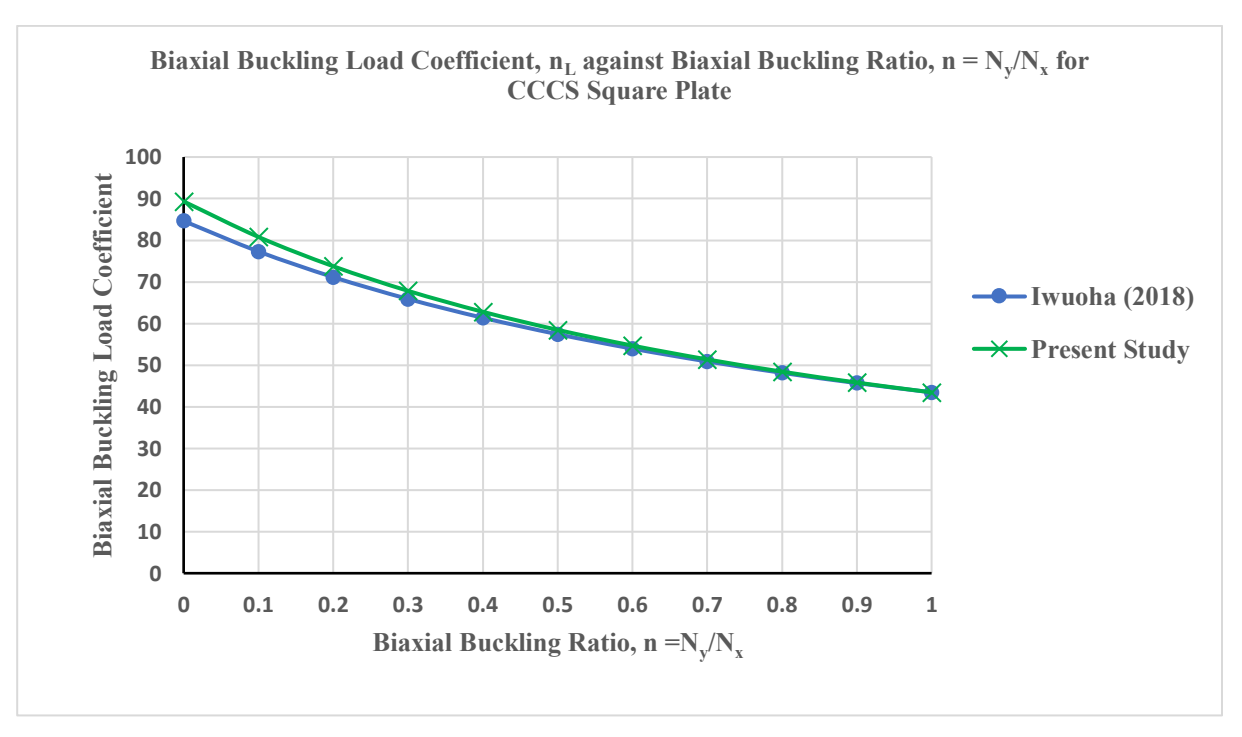


Fig 1: Graph of Critical Biaxial Buckling Load Coefficient, nLs, against Biaxial Buckling Ratio, n = Ny/Nx for CCCS Square Plate

From this Figure 1, it is shown that the present values are in very closed agreement with the ones compared. It further validates the adequacy of the new model for CCCS plate in particular and by extension others considered in this work since all were based on (5). The comparison of the biaxial buckling load coefficient, n_{sx} obtained in this study with that reported by [17] who applied Galerkin method reveals a percentage difference ranging from 0% to 5.56%, with the present study's results consistently upper bound of the range. The slight variation observed can be attributed to differences in the analytical methodologies adopted in deriving the solutions and approximations of numerical values. Nevertheless, the close numerical agreement between both sets of results demonstrates

the reliability of the present approach, with the deviation falling well within acceptable engineering and design tolerance limits.

To further validate these models, Table 13 shows a comparison of the values of the uniaxial buckling and postbuckling load coefficient (η_{Lx}) with those of [16] and [21] for a plate simply supported all-around (SSSS). The comparison with [16] showed a minimal deviation. The percentage difference increases with increase in w/t. This minor deviation is due completely to approximation of numerical values especially the number of decimal places adopted by the two authors for stiffness values. The result indicated that the present work is adequate. Moreso, the comparison with the classical work which has been acclaimed by many authors as a good

contribute to knowledge in large deflection analysis [22], [32], it indicated a maximum percentage difference of 22% at w/t of 2.303. This deviation may be due to the numerous assumptions and approximations used by Levy in his classical work to simply the process of getting solution to a very difficult problem of solving the von Karman large deflection equations. Besides, Levy used assumed trigonometric deflected shape function in his work, while this work used derived polynomial shape functions that gives clear mathematical justification to the

present result than that of Levy. To further discuss this deviation, Figure 2 shows a projected comparison of the percentage differences. From the Figure 2, it is clear the percentage difference trend of Levy demonstrates a diminishing return effect with the tendency of negligible deviation as the w/t increases. This is a clear indication that the present model is adequate and an improved model for stability analysis of thin isotropic plates.

Table 14: Comparison of the values of the Coefficient of Uniaxial Buckling and Postbuckling Load Coefficient (H $_{Lx}$) with those in Literature for SSSS Plate.

			η_{Lx}		
w t	Present study C ₁	Ibearugbulem et al. (2020) C_2	Levy (1942) C ₃	%Diff 100 $\frac{(c_1-c_2)}{c_2}$	%Diff 100 $\frac{(c_1-c_3)}{c_3}$
0	39.51	39.43	39.53	0.20	-0.07
0.25	40.69	40.61	40.18	0.18	1.26
0.498	44.20	44.07	42.77	0.29	3.33
0.743	49.95	49.69	46.88	0.54	6.56
0.984	57.83	57.36	52.60	0.83	9.94
1.22	67.68	66.97	59.52	1.05	13.71
1.45	79.30	78.42	68.05	1.12	16.53
1.673	92.48	91.27	77.99	1.32	18.58
1.889	107.04	105.53	89.01	1.43	20.26
2.101	123.05	121.20	101.32	1.53	21.45
2.303	139.89	137.61	114.61	1.65	22.06
2.498	157.61	155.00	129.51	1.68	21.69
2.687	176.15	173.04	145.61	1.80	20.98
2.871	195.51	192.05	161.70	1.80	20.91
3.044	214.88	210.96	181.36	1.86	18.48
3.212	234.77	230.40	202.75	1.89	15.79
3.376	255.22	250.38	231.70	1.93	10.15

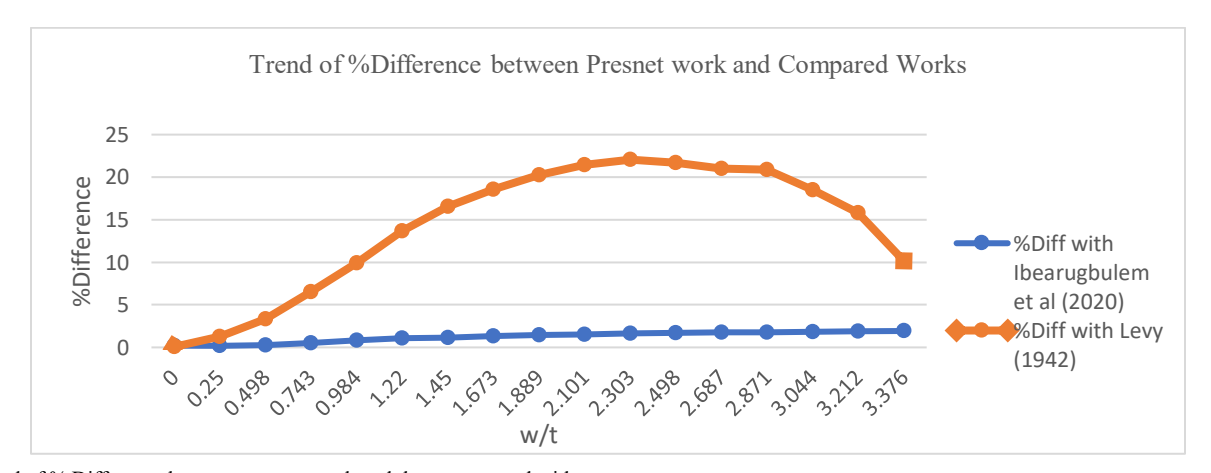


Fig 2: Trend of % Difference between present work and those compared with.

Tables 15 and 16 presents the biaxial load coefficient for CCCC and CCCS respectively for aspect ratio of 1.5. Comparing the biaxial buckling coefficients in Tables 7 and 15

for CCCC for aspect ratio 1 and 1.5 respectively, shows that, an increase in the aspect ratio of a CCCC reduces the strength of the plate. For instance, the critical load reduces from 108.000 to

60.963. This is 43.55% reduction in strength of the plate. This reduction in strength is due to increase deflection as a result of increase span length of the plate which reduces the plate's stiffness and its ability to resist in-plane loads. Similarly, looking at the biaxial buckling coefficients in Tables 11 and 16 for CCCS for aspect ratio of 1 and 1.5 respectively, shows a reduction of the critical load coefficient values from 89.333 to 40.424. This represents a 55% reduction in strength of a CCCS plates due to 0.5 increase in the aspect ratio of the plate. Furthermore, the effect of boundary condition on the strength of a plate can be seen when you look at the values of CCCC plate in Table 13 and those of CCCS plate in Table 16. The biaxial buckling values obtained in Table 15 and higher than those present in Table 16. The implication is that replacing one fixed support with a simple support reduces the strength of the plate. For instance, the critical load of CCCC plate from Table 15 is

60.963 as against 40.424 in Table 16 for CCCS plate. This means replacing one fixed support with a simple support reduces the strength of the plate by about 34%. All these have practical design considerations. It means that a plate's edge support types influence its strength or load resistance capacity.

From the results and discussions above, it is clear that the new models for each plate is adequate and robust to analyze both small and large deflection of thin isotropic rectangular plates. A look at the new equations suggest that the equations are applicable to a wide range of plate materials. What is required is to use the Young's modulus and Poisson ratio values of the material of interest. This will reduce difficulties of formulating different equations for different plate materials.

TABLE 15: BIAXIAL BUCKLING LOAD COEFFICIENT FOR CCCC PLATE WITH ASPECT RATIO OF 1.5

						ղւ					
n w/t	0	0.1	0.2	0.3	0.4	0.5	0.6	0.7	0.8	0.9	1
0	60.963	58.369	55.986	53.791	51.761	49.879	48.129	46.497	44.973	43.545	42.205
0.1	61.072	58.473	56.087	53.887	51.854	49.968	48.215	46.580	45.053	43.623	42.281
0.2	61.399	58.787	56.387	54.176	52.131	50.236	48.473	46.830	45.295	43.857	42.507
0.3	61.945	59.309	56.888	54.657	52.594	50.682	48.904	47.246	45.697	44.246	42.885
0.4	62.708	60.040	57.589	55.331	53.243	51.307	49.506	47.828	46.260	44.791	43.413
0.5	63.690	60.979	58.490	56.197	54.076	52.110	50.281	48.577	46.984	45.493	44.093
0.6	64.889	62.128	59.592	57.255	55.095	53.091	51.228	49.492	47.869	46.349	44.923
0.7	66.307	63.485	60.894	58.506	56.298	54.251	52.348	50.573	48.915	47.362	45.905
0.8	67.943	65.052	62.397	59.950	57.687	55.590	53.639	51.821	50.122	48.531	47.037
0.9	69.797	66.827	64.099	61.586	59.262	57.107	55.103	53.235	51.490	49.855	48.321
1	71.869	68.811	66.002	63.414	61.021	58.802	56.739	54.816	53.018	51.335	49.756

TABLE 16: BIAXIAL BUCKLING LOAD COEFFICIENT FOR CCCS PLATE WITH ASPECT RATIO OF 1.5

	η_{Lx}												
n w/t	0	0.1	0.2	0.3	0.4	0.5	0.6	0.7	0.8	0.9	1		
0	40.424	38.612	36.956	35.437	34.037	32.743	31.545	30.431	29.393	28.423	27.515		
0.1	40.558	38.741	37.079	35.554	34.150	32.852	31.650	30.532	29.490	28.518	27.607		
0.2	40.962	39.127	37.448	35.908	34.490	33.179	31.965	30.836	29.784	28.802	27.882		
0.3	41.635	39.769	38.064	36.498	35.057	33.724	32.490	31.342	30.273	29.275	28.340		
0.4	42.577	40.669	38.925	37.324	35.850	34.487	33.225	32.051	30.958	29.937	28.981		
0.5	43.788	41.826	40.032	38.386	36.869	35.468	34.170	32.963	31.839	30.789	29.805		

0.6	45.268	43.240	41.385	39.683	38.116	36.667	35.325	34.078	32.915	31.829	30.813
0.7	47.018	44.911	42.985	41.217	39.589	38.084	36.690	35.395	34.187	33.059	32.004
0.8	49.036	46.839	44.830	42.987	41.289	39.720	38.265	36.914	35.655	34.479	33.378
0.9	51.324	49.024	46.922	44.992	43.215	41.573	40.051	38.636	37.318	36.087	34.935
1	53.881	51.467	49.259	47.233	45.368	43.644	42.046	40.561	39.177	37.885	36.675

V. CONCLUSION

In this study, the biaxial stability equations for rectangular plates with CCCC, CSSS, CSCS, CCSS, CCCS and SSSS boundary conditions with large deflection conditions have successfully been formulated. The derived equations are sufficient to be applied in determining both biaxial and uniaxial buckling and postbuckling responses and are valid for cases involving either small or large deflections for each plate boundary condition considered in this study. Furthermore, the bending stiffnesses, membrane stiffnesses, and geometric load stiffnesses for each plate configuration have been explicitly evaluated, providing critical parameters for the structural analysis and design of plate elements. The critical buckling load coefficients for the aforementioned plate types can be determined for a range of aspect ratios and biaxial buckling ratios, offering valuable data for practical engineering applications. The validity of the present equations has been verified through comparison with previous studies, with the results showing only minimal deviations from those reported by other authors. This high level of agreement confirms the statistical reliability and engineering adequacy of the developed models, establishing a dependable analytical tool for predicting the buckling behaviour of these thin isotropic rectangular plates under study. This work has provided new equations for six plate types based on boundary conditions which will simplify thin plate analysis and design. This work has also, shown that (5) has a wider application for difference boundary condition in as much as the deflected shape function of such plate condition can be derived or is known. Moreso, this work has demonstrated the effect of boundary conditions on the strength of a plate. In addition, this work has provided useful numerical data for use in design and research. Finally, it has opened a research window for further studies and applicability of these models to such materials like Fibre Reinforced Polymer composite and other improved materials

ACKNOWLEDGMENT

We thanked the department of Civil Engineering, University of Cross River State, for creating enabling environment for this work to be carried out.

REFERENCES

- V. Birman, "Plate Structures" Springer Science & Business Media, vol. 178, 2011.
- [2] K. J. Sohn, and J. H. Kim, "Structural stability of functionally graded panels subjected to aero-thermal loads" Composite Structures, vol 82(3), pp 317– 325, 2008, https://doi.org/10.1016/J.COMPSTRUCT.2007.07.010
- [3] S. Chung Kim Yuen, G. N. Nurick, G. S. Langdon, and Y. Iyer, "Deformation of thin plates subjected to impulsive load: Part III an update 25 years on" International Journal of Impact Engineering, vol 107, pp 108–117, 2017. https://doi.org/10.1016/J.IJIMPENG.2016.06.010
- [4] T. Wierzbicki and G. N. Nurick, "Large deformation of thin plates under localised impulsive loading" International Journal of Impact Engineering,

- vol 18 (7–8), pp 899–918, 1996. https://doi.org/10.1016/S0734-743X(96)00027-9
- [5] B. Yang, C. G. Soares and D. Y. Wang, "Dynamic ultimate compressive strength of simply supported rectangular plates under impact loading" Marine Structures, vol 66, pp 258–271, 2019. https://doi.org/10.1016/J.MARSTRUC.2019.05.001
- [6] E. Ventsel, T. Krauthammer and E. Carrera "Thin Plates and Shells: Theory, Analysis, and Applications" Applied Mechanics Reviews, vol 55(4), pp B72–B73, 2002. https://doi.org/10.1115/1.1483356
- [7] M. Sathyamoorthy, "Nonlinear analysis of structures. In Nonlinear Analysis of Structures" CRC Press, 2017, https://doi.org/10.1201/9780203711255
- [8] O. A. Bauchau, and J. I. Craig, "Kirchhoff plate theory. In Structural Analysis" Springer Netherlands, pp. 819–914. 2009. https://doi.org/10.1007/978-90-481-2516-6 16
- [9] A. T. Zehnder and M. J. Viz "Fracture Mechanics of Thin Plates and Shells Under Combined Membrane, Bending, and Twisting Loads" Applied Mechanics Reviews, vol 58(1), pp 37–48, 2005). https://doi.org/10.1115/1.1828049
- [10] S. Ghuku, and K. N. Saha, "A review on stress and deformation analysis of curved beams under large deflection" International Journal of Engineering and Technologies, vol 11, pp 13–39, 2017. https://www.researchgate.net/profile/Kashinath-Saha/publication/318588632_A_review_on_Stress_and_Deformation_Analysis_of_Curved_Beams_under_Large_Deflection/links/5975a1c7a6 fdcc83488e9229/A-Review-on-Stress-and-Deformation-Analysis-of-Curved-Beams-under-Large-Deflection.pdf
- [11] Y. B. Yang, J. D. Yau and L. J. Leu, "Recent developments in geometrically nonlinear and postbuckling analysis of framed structures" Applied Mechanics Reviews, vol 56(4), pp 431–449, 2003.
- [12] W. S. Yoo, J. H. Lee, S. J. Park, J. H. Sohn, D. Pogorelov, and O. Dmitrochenko, "Large deflection analysis of a thin plate: Computer simulations and experiments" Multibody System Dynamics, vol 11(2), 185–208, 2004. https://doi.org/10.1023/B:MUBO.0000025415.73019.BB/METRICS
- [13] S. Timoshenko and S. Woinowsky-Krieger, "Theory of plates and Shells", McGraw-Hill Book Company, Inc.: New York, NY, USA, 1959.
- [14] H. Dai, X. Yue and S. Atluri, "Solutions of the von Kármán plate equations by a Galerkin method, without inverting the tangent stiffness matrix". Journal of Mechanics of Materials and Structures, vol 9(2), pp 195–226, 2014. https://msp.org/jomms/2014/9-2/p04.xhtml
- [15] D. O. Onwuka, O. M., Ibearugbulem and E. I. Adah, "Stability analysis of axially compressed SSSS & CSCS plates using MATLAB programming". International journal of science and technoledge, vol 4(1), pp 66-71, 2016
- [16] O. M. Ibearugbulem, E. I. Adah, D. O. Onwuka and C. E. Okere, "Simple and Exact Approach to Post-Buckling Analysis of Rectangular Plate" International Journal of Civil Engineering, Vo vol 7(6), pp 54–64, 2020. https://doi.org/10.14445/23488352/IJCE-V7I6P107
- [17] S. Iwuoha, "Biaxial Buckling Coefficients of Thin Rectangular Isotropic Plates, Having One Edge Simply Supported and the Other Edges Clamped" International Journal of Scientific & Engineering Research, vol 9(7), (2018).https://www.academia.edu/66030652/Biaxial_Buckling_Coefficients of Thin Rectangular Isotropic Plates Having One Edge Simply
- [18] I. Mascolo, "Recent Developments in the Dynamic Stability of Elastic Structures" Frontiers in Applied Mathematics and Statistics, vol 5, pp 487-546, 2019. https://doi.org/10.3389/FAMS.2019.00051/BIBTEX

_Supported_And_The_Other_Edges_Clamped?uc-g-sw=55422246

- [19] P. Moreno-García, J. V. A. dos Santos and H. Lopes, "A Review and Study on Ritz Method Admissible Functions with Emphasis on Buckling and Free Vibration of Isotropic and Anisotropic Beams and Plates" Archives of Computational Methods in Engineering, vol 25(3), pp 785–815, 2018. https://doi.org/10.1007/S11831-017-9214-7/METRICS
- [20] D. Onwuka, O. Ibearugbulem, S. Iwuoha, J. Arimanwa, and S. Sule, "Buckling Analysis of Biaxially Compressed All-Round Simply Supported (SSSS) Thin Rectangular Isotropic Plates Using the Galerkin's Method" Journal of Civil Engineering Urban, vol 6(3), pp 48–53, 2016).
- [21] S. Levy, "Bending of rectangular plates with large deflections". Technical notes: National Advisory Committee for Aeronautics (NACA), No. 846, 1942.
- [22] O. A. Oguaghamba, J. C. Ezeh, M. O. Ibearugbulem, and L. O. Ettu, "Buckling and Postbuckling Loads Characteristics of All Edges Clamped Thin Rectangular Plate" The International Journal of Engineering and Science, vol 4(11), pp 55–61, 2015. https://www.academia.edu/19492002/Buckling_and_Postbuckling_Load s Characteristics of All Edges Clamped Thin Rectangular Plate
- [23] E. I., Adah, O. M. Ibearugbulem, C. F. Ezeanyagu and E. E. Okon, "An Improved Formulation of Nonlinear Strain-Displacement Relations and Specific Mathematical Models for Stability Analysis of Thin Rectangular Plates", Journal of Inventive Engineering and Technology (JIET), vol 3(3), 85–102, 2023.
- [24] H. U. Edubi, "Biaxial Buckling Analysis of Thin Rectangular Plates under Large Displacement". An M. Eng. Thesis, submitted to the Department of Civil Engineering, University of Cross River State, 2025. (Unpublished).
- [25] O. M. Ibearugbulem, L. O. Ettu, and J. C. Ezeh, "Direct Integration and Work Principle as a New Approach in Bending Analyses of Isotropic

- Rectangular Plates". The International Journal of Engineering and Science, vol2(3), pp 28-36, 2013.
- [26] O. M. Ibearugbulem, J. C. Ezeh, and L. O. Ettu, "Energy Methods in Theory of Rectangular Plates (Use of Polynomial Shape Function)". Liu House of Excellence Ventures, Owerri, 2014.
- [27] O. M. Ibearugbulem, J. C. Ezeh, and L. O. Ettu, "Vibration Analysis of Thin Rectangular SSSS Plate using Taylor-Maclaurin Shape Function". International Journal of Academic Research, vol 4(6), 2012.
- [28] K. O. Njoku, J. C. Ezeh, O. M. Ibearugbulem, L. O. Ettu, and L. Anyaogu, "Free vibration Analysis of Thin Rectangular Isotropic CCCC plate using Taylor Seriess Formulated Shape Function in Galerkin's Method". Academic Research International Part-1: Natural and Applied Science, vol 4(4), pp 126-132, 2013.
- [29] D. O. Onwuka, O. M. Ibearugbulem, and U. G. Eziefula, "Plastic Buckling of SSSS Thin Rectangular Plates Subjected to Uniaxial compression using Taylor-Maclaurin Shape Function". Int. J. Struct. & Civil Engg. Res. Vol 2(4), pp 168-174, 2013.
- [30] U. G. Eziefula, O. M. Ibearugbulem, and D. O. Onwuka, "Plastic Buckling Analysis of an Isotropic C-SS-SS-SS Plate under in-plane Loading using Taylor's series Displacemnt Function". International Journal of Engineering and technology, vol 4(1), pp 17-22, 2014.
- [31] E. I., Adah, D. O. Onwuka and O. M. Ibearugbulem, "Development of polynomial-based program for pure bending analysis of SSSS rectangular thin isotropic plate" International Journal of science, engineering and technological research, vol 5(7), pp 2290-2295, 2016.
- [32] E. Ventsel and T. Krauthammer, "Thin plates and Shells: Theory, Analysis and Applications" New York, Marcel Dekker, 2001.